



**HAL**  
open science

## Study on thermal infrared emission directionality over crop canopies with TIR camera imagery

Qinhuo Liu, Xingfa Gu, Xiaowen Li, Frédéric Jacob, J F Hanocq, M. Friedl, A H Strahler, Tao Yu, Guoliang Tian

► **To cite this version:**

Qinhuo Liu, Xingfa Gu, Xiaowen Li, Frédéric Jacob, J F Hanocq, et al.. Study on thermal infrared emission directionality over crop canopies with TIR camera imagery. Science in China Series E: Technological Sciences, 2000, 43 (S1), pp.95-103. 10.1007/BF02916583 . hal-03735757

**HAL Id: hal-03735757**

**<https://hal.science/hal-03735757>**

Submitted on 22 Jul 2022

**HAL** is a multi-disciplinary open access archive for the deposit and dissemination of scientific research documents, whether they are published or not. The documents may come from teaching and research institutions in France or abroad, or from public or private research centers.

L'archive ouverte pluridisciplinaire **HAL**, est destinée au dépôt et à la diffusion de documents scientifiques de niveau recherche, publiés ou non, émanant des établissements d'enseignement et de recherche français ou étrangers, des laboratoires publics ou privés.

# Study on thermal infrared emission directionality over crop canopies with TIR camera imagery

LIU Qinhuo (柳钦火)<sup>1, 3</sup>, GU Xingfa (顾行法)<sup>2</sup>, LI Xiaowen (李小文)<sup>3, 4</sup>, F. Jacob<sup>2</sup>, J. F. Hanocq<sup>2</sup>, M. Friedl<sup>3</sup>, A. H. Strahler<sup>3</sup>, YU Tao (余涛)<sup>1</sup> & TIAN Guoliang (田国良)<sup>1</sup>

1. Laboratory of Remote Sensing Information Sciences, Chinese Academy of Sciences - Beijing 100101, China;
2. INRA-Unite De Bioclimatology, Avignon, France;
3. Center for Remote Sensing, Boston University, Boston, MA 02215, USA;
4. Center for Remote Sensing and GIS, Beijing Normal University, Beijing 100875, China Correspondence should be addressed to Liu Qinhuo (email: qhliu@irsa.irsa.ac.cn)

**Abstract** In order to investigate directionality of thermal infrared emission from crop canopies, a wide-angle thermal video camera (INFRAMETRICS) equipped with an 80° FOV lens was mounted on a small aircraft and used to acquire thermal imagery along several different flight traces. Accordingly, multi-angle directional brightness temperatures were acquired at different view angles for individual pixel. The flight experiment was carried out from January 1997 to October 1997 over a 5 km×5 km flat agricultural area, located near Avignon, southeastern France.

This paper presents results from analyses performed using these data including instrument calibration, radiometric correction, atmospheric correction, temperature temporal adjustment, geometric matching and registration of images. Results are presented for different thermal infrared emission patterns of different surface types including bare soil, wheat, maize and sunflower at different growth stages.

**Keywords:** TIR emission directionality, airborne experiment, crop canopy

Land surface temperature (LST) is a dynamic thermal equilibrium parameter in land-atmosphere interaction, which strongly depends on the micrometeorological conditions and water status of the surface. Up to now, the problem of non-isothermal pixel and angular dependence of the land surface temperature have remained to be solved<sup>[1-3]</sup>. In order to improve the knowledge of the thermal infrared emission directionality, experimental research work is accumulating, most of which is to measure directional brightness temperature of land surface targets with thermal infrared radiation (TIR) radiometer<sup>[4-12]</sup>. However, measuring directional surface temperature with TIR radiometer in field have the following problems: 1) The size and shape of radiometer view field change while TIR radiometer aims at targets with different view angles; 2) We have to face the challenge of space scale effect as the IR radiometer and remote sensors have quite different view fields; 3) As land surface temperature is a dynamic thermal equilibrium parameter, it will be affected by atmosphere turbulence and local meteorological conditions while the directional measurement takes several minutes.

In order to investigate the directional variability in the thermal emission of agricultural canopies, a wide-angle thermal video camera INFRAMETRICS, equipped with an 80° FOV lens, was perpendicularly mounted on a small aircraft during the experiment of the European remote sensing project ReSeDA. The camera has image acquisition ability of 25 frames per second. When aircraft flies over crop canopy along different flight directions in a short interval, the directional brightness temperature of individual pixel at different view angles and different sun geometrical configurations are acquired. This paper is to describe the preprocessing of the airborne TIR imagery. In order to extract the thermal infrared directionality information from the airborne TIR imagery, we have to remove out the measurement deviation result from instrument deterioration, atmospheric attenuation, geometric deformation, and temporal drifting. Then, we extract the TIR emission directional information of several typical crop canopies. The results help to improve our knowledge of the directionality of thermal infrared emission from several typical crop canopies.

## 1 Experiment description

## 1.1 Experiment site

The Alpilles ReSeDA test site is a 5 km×5 km area, located near Avignon (southeast of France), in the Rhone Valley. The latitude is 43°46' N and longitude is 4°45' E. It is a flat area surrounded by low altitude hills on the southern (Alpilles chain) and northwestern (Frigolet hill) sides. The main crops are wheat (32%), sunflower (20%), corn (9%), and grassland (16%). Fields are large enough (200 m×200 m) to extract pure pixels from high spatial resolution TIR camera image.

## 1.2 Data acquisition

### 1.2.1 Airborne data.

The instrument used is a thermal infrared camera INFRAMETRICS 760, which may operate in three wavebands equipped with three different filters (F1: 7.6—12.6  $\mu\text{m}$ , F2: 9.6 — 12.6  $\mu\text{m}$ , F3: 9.9 - 11.3  $\mu\text{m}$ ). In this experiment, filter F1 was selected (see fig. 1). The HgCdTe detector of the TIR camera works at 77 K with radiometric resolution of 0.2 to 0.4 degree. The camera's image acquisition rate is 25 frames per second with 230 lines by 362 columns. When it is implemented on a small airplane or a helicopter mounted with an 80° optic lens, a series of successive images with high overlap rate could be acquired. The view zenith angle of the image pixel increases from 0° at nadir up to 40° at off-nadir, while the view azimuth angle changes from 0° to 360° depending on the pixel location related to the nadir pixel (see Plate I-1).

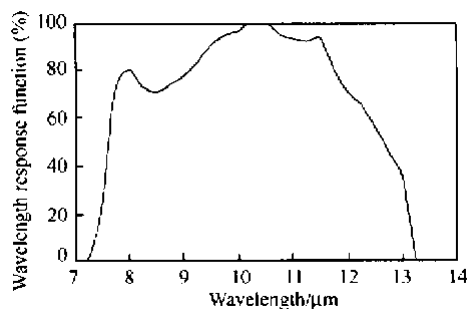


Fig. 1. Map of the experiment site.

The directional brightness temperatures of one individual pixel are available since its locations in a series of successive images are different.

During the experiment period, there were about total 22 airborne flights carried out from January 30, 1997 to September 18, 1997, which covered the growth period of several typical crops in these areas. The thermal camera was most of the time coupled with POLDER, with flight altitude of 3000 m. However, additional flights were performed using only the thermal camera with flight altitude of 1500 m. The spatial resolutions are respectively 20 and 10 meters. The flight speed is about 50 m/s. All the imageries have been digitized at a sampling frequency of 1 Hz (one image per second). At each date, the camera was operated along several flight axes covering the site: 3 to 5 axes being parallel to the solar plane and one axis being perpendicular. All the flights were carried out when it was clear and wind speed was low around the noon.

### 1.2.2 Ancillary data.

From January to October 1997, permanent monitoring of energy balance processes was carried out over some selected fields, covering the main crops encountered in the experimental area and spatially distributed over it. Measurements of vegetation structure were also regularly performed on the selected fields. The ancillary measurements mainly include the following items:

- Field measurement data: Leaf emissivity and soil emissivity; leaf reflectance and ground reflectance; canopy structure and biomass; canopy gap function and leaf area index; soil surface moisture and roughness.
- Flux measurement: heat flux and water vapor flux.
- Meteorological observation: Global, diffuse, long-wave and net radiation; air temperature at 2 m height; vapor pressure at 2 m height; wind speed and direction at 2 m height; soil temperature at 0.1, 0.5, 1.0 m; atmospheric pressure.
- Atmosphere characteristics: the radio-sounding data from the Nimes-Courbesac airport which is about 40 km from the experimental site and additional radio-sounding data by Météo-France.

## 2 Data preprocessing

### 2.1 Instrument calibration

Periodic calibrations of the camera were performed during the experiment campaign<sup>1</sup>. The calibration experimental protocol is as the follows. Sensor-target system is radiometrically isolated and sensor aims at a black body (water surface) during three hours, at a distance defined in order to avoid heat perturbations from target on lens and perturbations from sensor. Water emissivity is close to unit. Three ambient temperatures (15, 25 and 35°C) and five target temperatures (15, 25, 35, 45, and 55°C) are selected while sensor internal temperatures are also recorded<sup>1</sup>.

The calibration model takes account of three variables: target temperature  $T_{bt}$ , SCNR temperature  $T_{sc}$  and sensor temperature  $T_{bs}$ :

$$T_{bt} = a \cdot T_{sc}^3 + b \cdot T_{bs}^3 + c \cdot T_{sc}^2 \cdot T_{bs} + d \cdot T_{sc} \cdot T_{bs}^2 + g \cdot T_{sc} \cdot T_{bs} + hT_{sc} + iT_{bs} + j, \quad (1)$$

here,  $T_{bt}$  is target temperature,  $T_{bs}$  is the sensor temperature, and  $T_{sc}$  is the SCNR temperature, a, b, c, d, g, h, i, and j are calibration coefficients.

### 2.2 Atmospheric correction for the airborne TIR imagery

As the TIR camera is a mono-channel sensor, atmospheric corrections are to be done with aid of radiative transfer model MODTRAN.

The radiation reaching the sensor includes three parts as the following equation expressed. The meanings of the three parts are respectively the surface radiation, the hemisphere atmospheric downwelling radiation reflected to the sensor, and the atmospheric upwelling radiation between the ground surface and the sensor.

$$L(\lambda, \theta, \varphi) = t_{0-h}(\lambda, \theta, \varphi) \left\{ L_s(\lambda, \theta, \varphi) + \iint_U \rho(\lambda, \theta, \varphi, \theta', \varphi') \cdot [L_{a\downarrow}(\lambda, \theta', \varphi') \cos \theta'] \sin \theta' d\theta' d\varphi' \right\} + L_{a0-h}(\lambda, \theta, \varphi), \quad (2)$$

here,  $\theta$ ,  $\varphi$  are respectively the view zenith angle and the azimuth angle;  $\theta'$ ,  $\varphi'$  are respectively the atmosphere downwelling radiation zenith angle and azimuth angle,  $t_{0-h}(\lambda, \theta, \varphi)$  is the atmospheric transmittance from the ground to the airborne sensor at the view directions ( $\varphi, \theta$ );  $L_s(\lambda, \theta, \varphi)$  is the surface radiation at the directions ( $\varphi, \theta$ ),  $\rho(\lambda, \theta, \varphi, \theta', \varphi')$  is the bidirectional reflectance at the incoming

<sup>1</sup> ReSeDA: Assimilation of multi-sensor and multi-temporal remote sensing data to monitor vegetation and soil functioning. Annual Report, April 1998.

directions  $(\varphi', \theta')$  and the reflective directions  $(\varphi, \theta)$ ,  $L_a(\lambda, \theta', \varphi')$  is the downwelling radiation of the whole layer atmosphere at the directions  $(\varphi', \theta')$ ,

$L_{a0-h}(\lambda, \theta, \varphi)$  is the atmospheric upwelling radiation between the ground and the sensor at the directions  $(\varphi, \theta)$ .

If we define the directional surface brightness temperature  $T_{B_{sur}}(\theta, \varphi)$  with the following equation,  $L_{BB}$  is the Blackbody's radiation function according to Plank's law.

$$L_{BB}(\lambda, T_{B_{sur}}(\theta, \varphi)) = L_s(\lambda, \theta, \varphi) + \iint_U \rho(\lambda, \theta, \varphi, \theta', \varphi') \cdot [L_{a\downarrow}(\lambda, \theta', \varphi') \cos\theta'] \sin\theta' d\theta' d\varphi'. \quad (3)$$

Then, we can rewrite eq. (2) as in the following:

$$L_{BB}(\lambda, T_{B_{sen}}(\theta, \varphi)) = L_{BB}(\lambda, T_{B_{sur}}(\theta, \varphi)) \cdot t_{0-h}(\lambda, \theta, \varphi) + L_{a0-h}(\lambda, \theta, \varphi). \quad (4)$$

As the TIR camera is a wide band sensor, we should integrate the MODTRAN output with the sensor spectral response function. Thus, we get

$$\begin{aligned} & \int_{7.25}^{13.25} L_{BB}(\lambda, T_{B_{sen}}(\theta, \varphi)) \cdot S(\lambda) d\lambda \\ &= \int_{7.25}^{13.25} L_{BB}(\lambda, T_{B_{sur}}(\theta, \varphi)) \cdot t(\lambda, \theta, \varphi, 0-h) \cdot S(\lambda) d\lambda + \int_{7.25}^{13.25} L_{BB}(\lambda, T_{Ba\downarrow}(\theta, \varphi, 0-h)) \cdot S(\lambda) d\lambda. \end{aligned} \quad (5)$$

With the radio sounding atmosphere profile data, we can calculate the atmospheric transmittance and the atmospheric upwelling radiation between the ground surface and the sensor with simulation of MODTRAN program. As the experimental area is small and the weather condition was very good when the flight experiment was carried out, it is reasonable to assume that the atmosphere is horizontally homogeneous. Therefore, we assume that atmospheric parameters only depend on the view angle and are independent of the azimuth angle. Therefore, we can get the directional surface brightness temperature after atmospheric correction. However, the view angle depends on the pixel location on the TIR camera image. If we calculate the atmospheric parameter for every pixel, the simulation calculation time is beyond what we could afford. So, we simulate for a set of view angles every day and regress the relationship between the parameters and the view angles.

### 2.3 Geometrical correction of the airborne TIR imagery

Analysis of the directional information from a series of images requires the registration of the images. Image registration is a process of determining the position of corresponding points in two images of the same scene. If the difference between the images is any combination of translation, rotation and scaling, then by determining the positions of a minimum of two corresponding points (known as the control points) in the images, we can register the images.

According to the characters of the multi-angular thermal infrared imagery, a multi-step automatic geometric registration methodology has been designed. The accuracy can reach one pixel, which can meet the need of directional brightness temperature extraction<sup>2</sup>.

---

<sup>2</sup> Liu, Q. H., Gu, X. F., Tian, G. L. et al, Correlation analyses and automatic merging of airborne multi-angular thermal infrared imagery, Journal of Remote Sensing, 2000, suppl., in press.

## 2.4 Directional thermal infrared information extraction

After preprocessing, the surface temperature of each pixel in every image is given. For one ground point, different surface temperatures at different view angles are gained due to several different flights, which have a successive sequence of images to cover the same ground point. We developed a program to automatically extract the directional TIR emission information. This information includes flight number, sequence number, pixel location, surface temperature, view angle, observation time, solar angle, etc.

### 2.4.1 Directional surface temperature.

As pixel sizes and pixel shapes are different when the view angles are different, it is impossible to get the directional information of exactly the same target. In order to minimize the deviation caused by the geometric correction, we selected a small window with 5 by 5 pixels as research unit to represent each field. The small window was carefully selected in the middle of fields with at least 50 m distance to the field edge. After all the images were geometrically corrected to merge with the standard images and once we caught the field center coordination from the standard polder image, we can read all the brightness temperatures of pixels in the surrounding window from all those corrected TIR images, which can cover the whole window. Both the average temperature and the standard deviation of the 5 by 5 window were calculated for all images. As the sensor aims the target at different view angles in different TIR images, we get the data set of directional brightness temperature of the selected field.

2.4.2 View angle. The view angle difference of pixels in the small window of one field is very small. It is reasonable to extract the angle of the window center to represent the field view angle. The view angle of each pixel has been calculated for the whole image before. The view azimuth angle is calculated with the following formula:

$$\phi = \begin{cases} \arctan\left(\frac{y_0 - y}{x_0 - x}\right) + 90, & (\text{if } x_0 - x > 0), \\ \arctan\left(\frac{y_0 - y}{x_0 - x}\right) + 270, & (\text{if } x_0 - x < 0), \\ 0, & (\text{if } x - x_0 = 0, y_0 - y \leq 0), \\ 180, & (\text{if } x - x_0 = 0, y_0 - y \geq 0), \end{cases}$$

where,  $x$  and  $y$  are coordination of the window center in the standard image selected for geometric correction;  $x_0$  and  $y_0$  are coordination of the optical center of the image after geometric correction.

### 2.4.3 Solar angle.

We calculated solar zenith angle and azimuth angle for every flight sequence according to flight time, latitude and longitude of experimental site. It took about 1 to 2 minutes in one flight trace, so the variation in this short period can be neglected.

## 2.5 Normalization for different flight traces

Beside diurnal variation, there are also high frequency temporal variation of surface temperature resulting from influence of turbulence, solar radiation, cloud, wind speed, etc., which are more complicated than the diurnal variation.

In order to normalize the directional brightness surface temperature of different flight traces, one perpendicular flight trace is designed together with several parallel flight traces. When two flight traces

intersect, view angles are the same at the crossing point. Thus, the directional surface temperatures should be kept unvaried if there was no temporal variation while the solar configuration variation during a short interval was neglected. This characteristic is employed for temperature normalization.

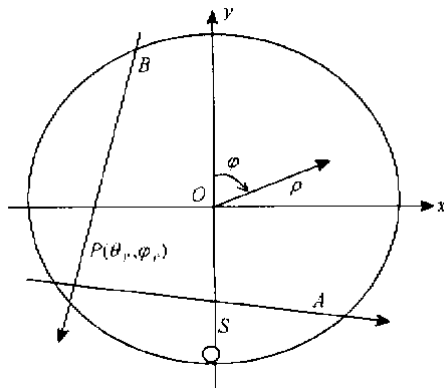


Fig. 2. Flight trace shown in polar coordinates.  $\rho$  equals zenith angle and  $\varphi$  equals azimuth angle, S is solar position, OS is the solar principal plane, PA is perpendicular to solar plane and PB is parallel to the solar plane and P is crossing point of two flight traces.

After we get the directional temperatures of every parallel plane and one perpendicular plane, we may present them in polar coordinate system. Define the radius  $\rho$  as zenith angle and rotation angle  $\varphi$  as azimuth angle. The coordinate system is clockwise with 0 at north (see fig. 2). After the coordinates  $(\theta_p, \varphi_p)$  of the crossing point P are calculated, we may normalize the directional surface temperature of different flight traces as follows:

$$T_N = T + (T_{P\perp} - T_{P\parallel}),$$

where  $T_{P\perp}$  and  $T_{P\parallel}$  are directional surface brightness temperatures of perpendicular and parallel planes at the crossing point P  $(\theta_p, \varphi_p)$ ,  $T_N$  is the normalized directional brightness temperature and T is the directional brightness temperature before normalization.

Plate I-2 shows directional brightness temperatures of parallel plane and perpendicular plane before and after being normalized. Plate I-2(a) is the view angle distribution of different flight traces. Plate I-2(b) shows the directional brightness temperature before being normalized and Plate I-2(c) the normalized directional brightness temperature. The same color represents the same flight trace in Plate I-2(a), (b), and (c). Before normalization, temperature differences among different flight traces due to the temporal effect are 1 to 2 degrees. After normalization, we can see that the directional brightness temperature distribution is more reasonable than before.

### 3 TIR directionality analyses

After normalization of the brightness temperatures, there are two presentation methods used to describe the directional thermal infrared emission information over the crop canopy here. One is the directional temperatures variation in the principal plane, which is helpful to showing the maximum temperature difference as the view angle changes in the solar plane. The other is the directional temperature distribution in all view zenith angles and azimuth angles while it is helpful to showing the directional brightness temperature distribution as view angle.

Data sets have been set up which include directional thermal infrared information of several typical surfaces from March to July 1997, which would be helpful for theoretical research. Some dates are selected to analyze the TIR emission directionality of crop area. Plate I-3 shows temperature differences in the planes parallel or perpendicular to solar principal plane on March 12, 1997. Plate I-4 shows the

directional brightness temperature distribution of several surface types vs. view zenith angle and azimuth angle. Plate I-5 expresses the directional brightness temperature distribution of winter wheat during different growth stages.

From the TIR directional distribution (Plate I-3 -5), we may draw some conclusions as follows:

TIR directionality depends on surface type, structure parameter and solar radiation, etc.

In the principal plane, the directional temperature differences can reach 3 to 4 degrees, while high temperature occurs in the backward direction.

In the perpendicular plane, the directional temperature differences are near symmetry. 'Hot spot' may exist but it is not exactly the backward direction with visual band.

#### 4 Conclusion and discussion

The TIR camera has fast image acquisition ability. When aircraft is equipped with wide FOV lens over crop canopy along different flight directions in a short interval, the directional brightness temperature of individual pixel at different view angles and different sun geometrical configurations are acquired. Airborne experiment has characters of high speed, large view field, which can simulate satellite remote sensing better than field experiment. It is significantly important to study the directionality of thermal infrared emission of land surface by airborne experiment.

This paper describes the preprocessing of airborne TIR imagery. In order to extract thermal infrared directionality information from airborne TIR imagery, it is necessary to remove out the measurement deviation resulting from instrument deterioration, atmospheric attenuation, geometric deformation and temporal drifting.

We extract TIR emission directional information of several typical crop canopies. Results help to improve our knowledge of the directionality of thermal infrared emission from several typical crop canopies. TIR emission directionalities from crop canopies are quite different in different growth stages. The mechanism of TIR emission directionality is complicated. The most important factors include: land surface structure, pixel component emissivity and component temperature distribution. As temperature structure in pixel closely relates to solar radiation, micro- meteorological condition and physics condition of land surfaces, the TIR emission directionalities change with season, time and other conditions.

Extensive experimental research is necessary for better understanding the TIR emission directional mechanism. Thermal infrared camera is a powerful instrument for acquisition of directional TIR imagery. We can improve the experiment protocol as follows:

Let TIR camera mounted on airplane be of oblique angle, so larger view zenith angle TIR image can be acquired.

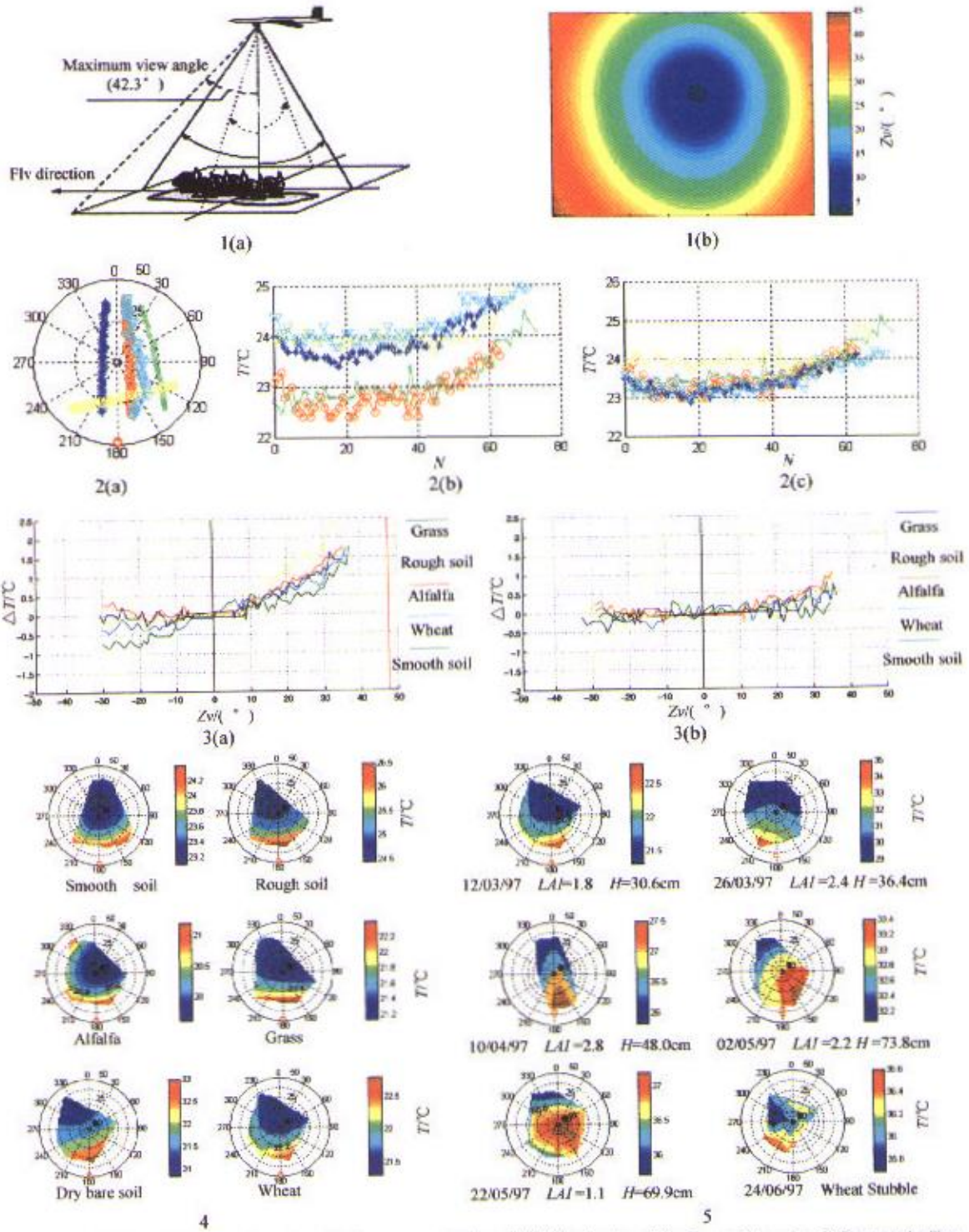
Design a flight scheme at night, so TIR image without solar radiation can be used to compare with the day-time image, which would be helpful to understanding the solar radiation's influence.

Acknowledgements This work was funded under China's Key-Important Basic Research Project (95-Y-38), China's Special Funds for Major State Basic Research Project (Grant No. 2000077900) and USA's NASA Project (NAG5-7217).

#### References

1. Hall, F. C., Huemmrich, K. F., Goetz, S. J. et al., Satellite remote sensing of surface energy balance: success, failures and unresolved issues in FIFE, *J. Geophys. Res.*, 1992, 97: 19061.

2. Liu, Q. H., Xu, X. R., Chen, J. Y., The retrieval of land surface temperature and emissivity by remote sensing data: Theory and digital simulation, *Journal of Remote Sensing (in Chinese)*, 1998, 2(1): 1.
3. Li, X., Strahler, A., Friedl, M., A conceptual model for effective directional emissivity from nonisothermal surface, *IEEE Trans. on Geosci. Remote Sensing*, 1999, 35(5): 2508.
4. Fuchs, M., Kuncm, E. T., Kcrr. J. P., Tanner, C.B., Effect of viewing angle on canopy temperature measurements with in- frared thermometers, *Agron. J.*, 1967, 59: 494.
5. Kimes, D. S., View angle effects in the radiometric measurement of plant canopy temperatures, *Remote Sensing Environ.*, 1980, 10: 273.
6. Huband, N. D. S., Monteith, J. L., Radiative surface temperature and energy balance of a wheat canopy: I. Comparison of radiative and aerodynamic canopy temperature, *Boundary Layer Meteorol.*, 1986, 36: 1.
7. Kimes, D. S., Remote sensing of row crop structure and component temperatures using directional radiometric tempera- tures and inversion techniques, *Remote Sensing of Environment*, 1983, 13: 33.
8. Pawu, K.T., Ustin, S. L., Zhang, C., Anisotropy of thermal infrared exitance in sunflower canopies, *Agric. For. Meteorol.*, 1989, 48: 45.
9. Mc Guire, M. J., Balick , L. K., Smith, J. A., Hutchinson, B. A., Modeling directional thermal radiance from a fovert can- opy, *Remote Sens. Environ.*, 1989, 27: 169.
10. Bailick, L. E., Hutchinson, B. A., Directional thermal infrared exitance distributions from a leafless deciduous forest, *IEEE. Trans. Geosci. Remote Sens.*, 1986, 24(5): 693.
11. Lagouarde, J.P., Kerr, Y.H. Brunet, An experimental study of angular effects on surface temperature for various plant canopies and bare soils, *Agricultural and Forest Meteorology*, 1995, 77: 167.
12. François, C., Otlé, L., Prévot, L., Analytical parameterization of canopy directional emissivity and directional radiance in the thermal infrared: Application on the retrieval of soil and foliage temperatures using two directional measurements, *In- ternational Journal of Remote Sensing*, 1997, 18(12): 2587.



1. View field and view zenith angle of TIR camera: (a) view field distribution, (b) view zenith angle. 2. Temporal effect normalization of directional brightness temperature (DBT): (a) view angle distribution, (b) DBT before normalization, (c) normalized DBT. 3. Relationship of directional brightness temperature vs view zenith angle: (a) principal plane, (b) perpendicular plane. 4. Directional brightness temperature of different surface types (12/03/97). 5. Directional brightness temperature distribution of wheat in different growth stages.